2010

Two-subband conduction in a gated high density InAlN/AlN/GaN heterostructure

H. Cheng
University of Michigan - Ann Arbor, hailingc@umich.edu

C. Kurdak
University of Michigan - Ann Arbor

J. H. Leach
Virginia Commonwealth University

M. Wu
Virginia Commonwealth University

Hadis Morkoç
Virginia Commonwealth University, hmorkoc@vcu.edu

Cheng, H., Kurdak, C., Leach, J.H. Two-subband conduction in a gated high density InAlN/AlN/GaN heterostructure. Applied Physics Letters, 97, 112113 (2010). Copyright © 2010 AIP Publishing LLC.

Two-subband conduction in a gated high density InAlN/AlN/GaN heterostructure

H. Cheng,[1,a)] Ç. Kurdak,[1] J. H. Leach,[2] M. Wu,[2] and H. Morkoç[2]
[1]*Department of Physics, University of Michigan, Ann Arbor, Michigan 48109, USA*
[2]*Department of Electrical and Computer Engineering, Virginia Commonwealth University, Richmond, Virginia 23284, USA*

(Received 3 May 2010; accepted 17 August 2010; published online 17 September 2010)

Magnetotransport measurements on an $In_{0.16}Al_{0.84}N/AlN/GaN$ gated Hall bar sample have been performed at 0.28 K. By the application of a gate voltage we were able to vary the total two-dimensional electron gas density from 1.83×10^{13} to 2.32×10^{13} cm^{-2}. Two frequency Shubnikov–de Haas oscillations indicate occupation of two subbands by electrons. The density of electrons in the first and second sublevels are found to increase linearly with gate voltage with a slope of 2.01×10^{12} cm^{-2}/V and 0.47×10^{12} cm^{-2}/V, respectively. And the quantum lifetimes for the first and second subbands ranged from 0.55 to 0.95×10^{-13} s and from 1.2 to 2.1×10^{-13} s.
 [doi:10.1063/1.3490248]

GaN heterostructures are being increasingly used in high frequency, and high temperature device applications.[1] One advantage of InAlN/GaN heterostructures[2–4] over traditional AlGaN/GaN heterostructures is the lattice match between the $In_{0.17}Al_{0.83}N$ barrier and the GaN layer, which is beneficial to reduce the strain in heterostructures to achieve high quality devices. The lattice matching molar fraction of InN in the barrier depends on the strain state of the GaN channel layer.[5] Furthermore, the spontaneous polarization difference between GaN and $In_{0.17}Al_{0.86}N$ is larger than that in the typical AlGaN/GaN heterostructures, which could result in a higher density two-dimensional electron gas (2DEG). In AlGaN/GaN heterostructures, the high carrier density regime has been studied previously and occupation of multiple subbands was observed.[6–8] A carrier density as high as 1.4×10^{13} cm^{-2} has been reported,[8] which was achieved in non-gated samples by using the persistent photoconductivity (PPC). When the PPC is used, the change of sample carrier density cannot be reversed at low temperatures and the non-uniformity of carrier density could be a potential issue affecting the Shubnikov–de Haas (SdH) measurements.

In this paper, we report two-subband conduction in a high carrier density gated $In_{0.16}Al_{0.84}N/AlN/GaN$ Hall bar sample. We changed the carrier density of the 2DEG by using a gate and the highest carrier density was 2.3×10^{13} cm^{-2}. We monitored the occupation of the two subbands using SdH oscillations. The density of electrons in both sublevels increased linearly with increasing gate voltage, but with different slopes, which is explained by an increase in the energy level separation between two subbands induced by the increasing gate voltage.

The InAlN/AlN/GaN (Refs. 9 and 10) sample was grown in an organometallic-vapor-phase epitaxy system on a sapphire substrate. A 250 nm initiation layer of AlN was followed by a 3.0 μm of undoped GaN. Due to contamination,[10] the sample growth was interrupted to change the sample holder. The growth was continued with a 100 nm GaN, followed by a 1 nm AlN, a 15 nm of $In_{0.16}Al_{0.84}N$ and a 2 nm GaN cap layer. Finally, the gated Hall bar (600×100 μm^2) was fabricated by photolithography.

The sample was characterized by magnetotransport measurements in He3 cryostat. In Fig. 1, we plot the low temperature magnetoresistance for the sample from −1.8 to 0 V gate bias. The sample exhibited clear SdH oscillations at 0.28 K and starting from −1.6 V, we observed well-pronounced two frequency SdH oscillations up to 0.4 V, a clear indication of two-subband occupation in the 2DEG (see the inset of Fig. 1). To separate the two frequency oscillation components from the data, we first plotted the data versus inverse magnetic field (1/B), then used fast Fourier transform to filter out the high and low frequency components and converted the data back to the B scale. Those two frequency components were fitted to a typical Dingle form[11] as

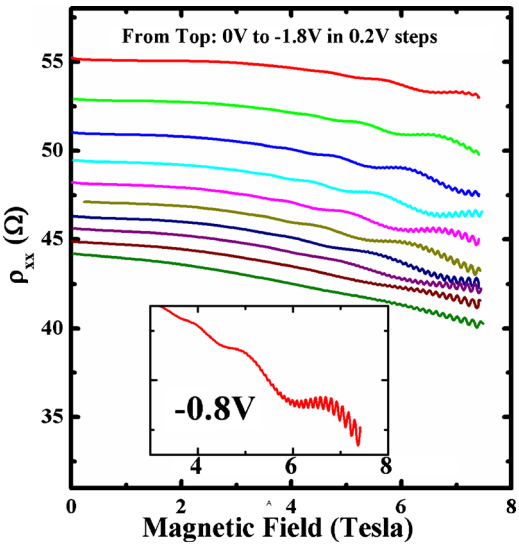

FIG. 1. (Color online) Longitudinal magnetotransport measurements at gate voltages from −0 to −1.8 V (from top to bottom in 0.2 V steps). The inset is the expanded data at $V_{gate}=-0.8$ V, which shows well-pronounced two frequency SdH oscillations.

a)Electronic mail: hailingc@umich.edu.

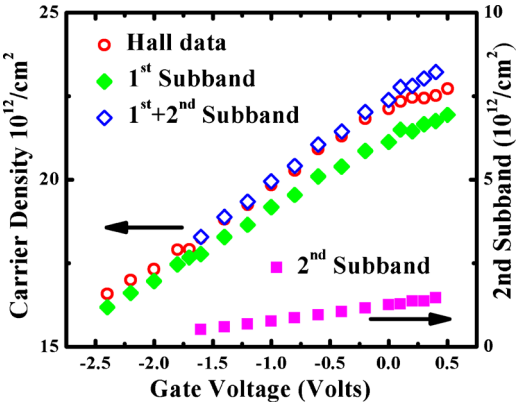

FIG. 2. (Color online) Carrier densities vs gate voltage. The solid dots are the carrier densities for 1st and 2nd subbands. Note that right scale is used for the 2nd subbands data. The hollow circles are the carrier densities extracted from Hall slope and the hollow diamonds are the sum of two subbands carrier densities.

$$\rho_{xx}(B) = A + C\exp\left(\frac{-\pi}{\omega\tau_q}\right)\frac{\xi}{\sinh(\xi)}\cos\left(\frac{2\pi\Delta E}{\hbar\omega} + \varphi\right), \quad (1)$$

where A, C, and φ are just fitting constants; B is the magnetic field; $\omega = eB/m^*$ is the cyclotron frequency; m^* is the effective mass[12] (0.23 m_e); τ_q is the quantum lifetime; $\xi = 2\pi^2 k_B T/(\hbar\omega)$; $\Delta E = \pi\hbar^2 n/m^*$ is the energy difference between Fermi level and the subband energy level, and n is the carrier density. For gate voltages from −1.4 to 0.4 V, we extracted τ_q, n, and ΔE for both 1st and 2nd subbands. In Fig. 2, we plot the carrier densities at different gate voltages. The solid data points represent the carrier densities for 1st and 2nd subbands extracted from the SdH oscillations. Also the sum of the two subbands and the carrier density extracted from Hall measurements (not shown) are plotted together for comparison. In the extraction we assumed that electrons in both sublevels had identical mobility. However, we see a small but noticeable deviation between the Hall data and the sum of two subbands, most likely due to the mobility difference in the two subbands.[13] We also plotted quantum lifetime versus gate voltage in Fig. 3. The 2nd subband exhibits quantum lifetimes τ_{2q} ranging from 1.2×10^{-13} to 2.1×10^{-13} s and the 1st subband exhibits quantum lifetimes τ_{1q} ranging from 0.55×10^{-13} to 0.95×10^{-13} s. Therefore we expect that the 2nd subband has a higher mobility than the 1st subband.

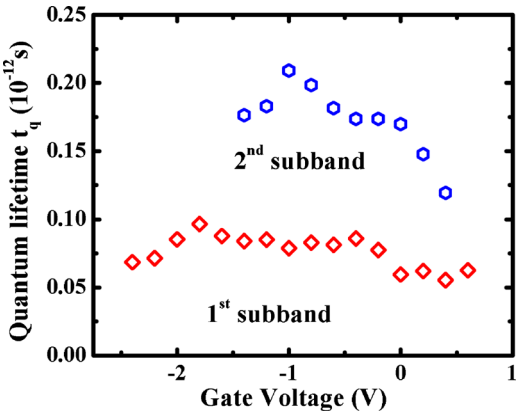

FIG. 3. (Color online) Quantum lifetime vs gate voltage for the two subbands.

The total carrier density in the 2DEG channel is the sum of 1st and 2nd subband's, which is found to vary with gate voltage linearly, consistent with a capacitance model. For gate voltages from −1.6 to 0.4 V, the total carrier densities are remarkably high, changing from 1.83×10^{13} to 2.32×10^{13} cm^{-2}, with errors less than 0.5% coming from the estimation of fast Fourier transform (FFT) peak positions. The second subband carrier density is much smaller and ranged from 0.51×10^{12} to 1.46×10^{12} cm^{-2}. When we extrapolate the data, we would expect to enter a single subband regime at a carrier density of 1.6×10^{13} cm^{-2}.

In 2DEG with multiple occupied subbands, the electron density in each sublevel is given by $n_i = m^*(E_F - E_i)/(\pi\hbar^2)$ where m^* is the effective mass, E_F is the Fermi energy, and E_i is the energy level in the i^{th} subband. The Fermi energy is expected to increase with addition of new electrons, which would be split equally among all the occupied sublevels. We note, however, that the electrons added into the 2DEG by increasing the gate voltage did not split equally between the two subbands. The change in the carrier densities of the 1st and 2nd subbands with respect to gate voltage dn_i/dV_g were 2.01×10^{12} cm^{-2}/V and 0.47×10^{12} cm^{-2}/V, respectively. Two-subbands conduction in an AlGaN/GaN heterostructure has been studied by using the PPC.[7] Interestingly most of the additional electrons provided by the PPC were observed to split between the 1st and 2nd subbands with a 4 to 1 ratio, which is close to that observed in our gated sample.

The uneven splitting of additional electrons among the subbands can arise from either the different effective mass of electrons or the variations in the confinement associated with gating. In low bandgap semiconductors,[14] the uneven splitting of additional electrons among subbands was attributed to different effective masses due to conduction band nonparabolicity. But in GaN, the nonparabolicity of the conduction band would not be significant. Therefore, we must focus on the possible shifts in the subband energy levels as the cause. In particular, an increase in the energy level separation between the two subbands, $E_{21} = E_2 - E_1$, with increasing gate voltage is needed to explain our data. We note that similar energy shifts in energy levels have been previously studied in AlGasAs/GaAs.[15,16] In the simplest case of an infinite triangular potential, E_{21} scales as $A^{2/3}$, where A is the slope of triangular potential.[17] When we increase the electron density, the confining potential changes in such a way as to increase the E_{21}. To support our premise, we performed ATLAS conduction band diagram simulations for different gate voltages. Figure 4 shows a plot of the subband energies calculated as well as extracted from measurements versus the gate voltage. The calculated energy levels agree with our experimental result quantitatively. From the calculation, we conclude that E_{21} increases with increasing gate voltage and it is the major contribution to the uneven splitting of added electrons.

The mobilities of electrons in the 1st and 2nd subbands are not expected to be the same.[13] The transport is mainly dominated by the electrons in the 1st subband due to its high concentration. Thus, we can only extract the mobility of the electrons in the 1st subband reliably. Considering the ratio of the quantum lifetimes was $\tau_{1q}/\tau_{2q} \sim 1/2$, we assumed that the ratio of momentum relaxation times was also $\tau_{1m}/\tau_{2m} \sim 1/2$, where τ_{im} is the momentum relaxation time for the i^{th} subbands. Following this assumption, we extracted the mobilities for the 1st subband ranging from 7400 to

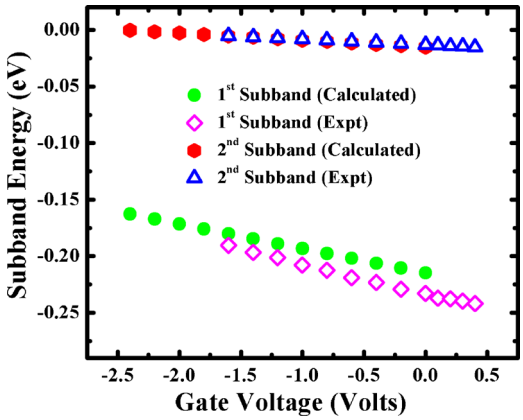

FIG. 4. (Color online) Subband energy vs gate voltage. Solid points are calculation results from ATLAS simulation and hollow points are experimental data. The Fermi energy is taken as the reference (E_F=0 eV).

4290 $cm^2/V\,s$ as the carrier density increased from 18.3 $\times 10^{12}$ to 23.2×10^{12} cm^{-2}. The mobilities extracted depends weakly on τ_{1m}/τ_{2m}; when we assumed $\tau_{1m}/\tau_{2m}=1$, the mobilities of the 1st subband ranged from 7610 to 4560 $cm^2/V\,s$. In high carrier density regime, the surface roughness and alloy scattering are expected to be the dominant scattering mechanisms which would lead to a decrease in electron mobility with increasing carrier concentration, consistent with our measurements. Finally, the momentum relaxation times are found to be an order of magnitude larger than the quantum lifetimes. This is typical since the quantum relaxation is sensitive to small angle scattering processes while the momentum relaxation is not.[11,16,18,19]

In summary, we have investigated magnetotransport properties of an $In_{0.16}Al_{0.84}N/AlN/GaN$ gated Hall bar sample at different gate voltages. Well-pronounced two frequency SdH oscillations have been observed due to the occupation of two subbands. Carrier densities and quantum lifetimes in those two subbands have been extracted from SdH oscillations and the highest total carrier density reaches 2.32×10^{13} cm^{-2}. We also observed different rate of change of the electron density versus the gate bias, dn/dV_g, in two subbands, which is explained by the increase in energy level separation between the first and the second subband induced by increasing gate voltage.

This work is supported by grants FA9550-09-1-0595 from the Air Force Office of Scientific Research under the direction of Dr. K. Reinhardt and by the NSF Grant Nos. DMR-0606039 and DMR-1006500.

[1]H. Morkoç, *Handbook of Nitride Semiconductors and Devices* (Wiley, New York, 2008), Vol. 3.
[2]J. W. Chung, O. I. Saadat, J. M. Tirado, X. Gao, S. P. Guo, and T. Palacios, IEEE Electron Device Lett. **30**, 904 (2009).
[3]M. Gonschorek, J. F. Carlin, E. Feltin, M. A. Py, N. Grandjean, V. Darakchieva, B. Monemar, M. Lorenz, and G. Ramm, J. Appl. Phys. **103**, 093714 (2008).
[4]J. Kuzmík, IEEE Electron Device Lett. **22**, 510 (2001).
[5]J. H. Leach, M. Wu, X. Ni, X. Li, Ü. Özgür, and H. Morkoç, Phys. Status Solidi A **207**, 211 (2010).
[6]Z. W. Zheng, B. Shen, R. Zhang, Y. S. Gui, C. P. Jiang, Z. X. Ma, G. Z. Zheng, S. L. Guo, Y. Shi, P. Han, Y. D. Zheng, T. Someya, and Y. Arakawa, Phys. Rev. B **62**, R7739 (2000).
[7]I. Lo, J. K. Tsai, M. H. Gau, Y. L. Chen, Z. J. Chang, W. T. Wang, J. C. Chiang, K. R. Wang, C.-N. Chen, T. Aggerstam, and S. Lourdudoss, Phys. Rev. B **74**, 245325 (2006).
[8]Z. W. Zheng, B. Shen, C. P. Jiang, Y. S. Gui, T. Someya, R. Zhang, Y. Shi, Y. D. Zheng, S. L. Guo, J. H. Chu, and Y. Arakawa, J. Appl. Phys. **93**, 1651 (2003).
[9]J. H. Leach, C. Y. Zhu, M. Wu, X. Ni, X. Li, J. Xie, U. Ozgur, H. Morkoc, J. Liberis, E. Sermuksnis, A. Matulionis, H. Cheng, and C. Kurdak, Appl. Phys. Lett. **95**, 223504 (2009).
[10]J. H. Leach, X. Ni, X. Li, M. Wu, H. Morkoç, L. Zhou, D. A. Cullen, D. J. Smith, H. Cheng, Ç. Kurdak, J. R. Meyer, and I. Vurgaftman, J. Appl. Phys. **107**, 083706 (2010).
[11]P. T. Coleridge, R. Stoner, and R. Fletcher, Phys. Rev. B **39**, 1120 (1989).
[12]A. M. Kurakin, S. A. Vitusevich, S. V. Danylyuk, H. Hardtdegen, N. Klein, Z. Bougrioua, A. V. Naumov, and A. E. Belyaev, J. Appl. Phys. **105**, 073703 (2009).
[13]H. L. Störmer, A. C. Gossard, and W. Wiegmann, Solid State Commun. **41**, 707 (1982).
[14]M. Ahoujja, S. Elhamri, R. S. Newrock, D. B. Mast, W. C. Mitchel, I. Lo, and A. Fathimulla, J. Appl. Phys. **81**, 1609 (1997).
[15]H. van Houten, J. G. Williamson, M. E. I. Broekaart, C. T. Foxon, and J. J. Harris, Phys. Rev. B **37**, 2756 (1988).
[16]R. Fletcher, E. Zaremba, M. D'Iorio, C. T. Foxon, and J. J. Harris, Phys. Rev. B **38**, 7866 (1988).
[17]J. H. Davis, *The Physics of Low-Dimensional Semiconductors: An Introduction* (Cambridge University Press, New York, 1998).
[18]S. Elhamri, R. S. Newrock, D. B. Mast, M. Ahoujja, W. C. Mitchel, J. M. Redwing, M. A. Tischler, and J. S. Flynn, Phys. Rev. B **57**, 1374 (1998).
[19]J. P. Harrang, R. J. Higgins, R. K. Goodall, P. R. Jay, M. Laviron, and P. Delescluse, Phys. Rev. B **32**, 8126 (1985).